Mapping the BK_{Ca} Channel's "Ca^{2+} Bowl": Side-chains Essential for Ca^{2+} Sensing

Lin Bao, Christina Kaldany, Ericka C. Holmstrand, and Daniel H. Cox

Molecular Cardiology Research Institute, New England Medical Center, and the Department of Neuroscience, Tufts University School of Medicine, Boston, MA 02111

ABSTRACT There is controversy over whether Ca^{2+} binds to the BK_{Ca} channel's intracellular domain or its integral-membrane domain and over whether or not mutations that reduce the channel's Ca^{2+} sensitivity act at the point of Ca^{2+} coordination. One region in the intracellular domain that has been implicated in Ca^{2+} sensing is the "Ca^{2+} bowl". This region contains many acidic residues, and large Ca^{2+}-bowl mutations eliminate Ca^{2+} sensing through what appears to be one type of high-affinity Ca^{2+}-binding site. Here, through site-directed mutagenesis we have mapped the residues in the Ca^{2+} bowl that are most important for Ca^{2+} sensing. We find acidic residues, D898 and D900, to be essential, and we find them essential as well for Ca^{2+} binding to a fusion protein that contains a portion of the BK_{Ca} channel's intracellular domain. Thus, much of our data supports the conclusion that Ca^{2+} binds to the BK_{Ca} channel's intracellular domain, and they define the Ca^{2+} bowl's essential Ca^{2+}-sensing motif. Overall, however, we have found that the relationship between mutations that disrupt Ca^{2+} sensing and those that disrupt Ca^{2+} binding is not as strong as we had expected, a result that raises the possibility that, when examined by gel-overlay, the Ca^{2+} bowl may be in a nonnative conformation.

KEY WORDS: mSlo • BK_{Ca} • potassium channel • Ca^{2+} bowl • Ca^{2+} binding

INTRODUCTION

The large-conductance Ca^{2+}-activated K^+ channel (BK_{Ca}) provides a link between chemical and electrical signaling by opening in response to micromolar concentrations of Ca^{2+} close to the plasma membrane (Latorre et al., 1989). The primary sequence of the channel's pore-forming (Slo) subunit, however—four of which form a fully functional channel—contains no established Ca^{2+} binding motifs (Atkinson et al., 1991; Adelman et al., 1992; Butler et al., 1993; Pallanck and Ganetzky, 1994), and so the origin of the BK_{Ca} channel's Ca^{2+} sensitivity has been of considerable interest as it likely involves structurally novel Ca^{2+}-binding sites.

Slo's secondary structure (Fig. 1) suggests that a large intracellular carboxy-terminal domain unique to this channel has evolved to confer Ca^{2+} sensitivity upon what is otherwise a voltage-gated K^+ channel (Butler et al., 1993; Wei et al., 1994; Schreiber et al., 1999). Indeed, the BK_{Ca} channel is considerably voltage sensitive (Barrett et al., 1982; Methfessel and Boheim, 1982), and mutations in its intracellular domain reduce and, in combination, eliminate its Ca^{2+} sensitivity (Schreiber and Salkoff, 1997; Bian et al., 2001; Bao et al., 2002; Xia et al., 2002). Contrary to this view, however, it has been found that the Slo subunit can be truncated just after its putative S6 helix, eliminating the channel's entire intracellular domain, and the resulting construct, although it expresses poorly, produces channels with near wild-type Ca^{2+} sensitivity (Piskorowski and Aldrich, 2002). This argues that the BK_{Ca} channel's Ca^{2+}-binding sites reside entirely in Slo's integral-membrane domain and therefore that mutations in the intracellular domain that affect Ca^{2+}-dependent channel opening must do so indirectly.

Despite this important result, however, there are still compelling reasons to think that the BK_{Ca} channel's intracellular domain might bind Ca^{2+}. First, the crystal structure of the bacterial Ca^{2+}-activated K^+ channel, MthK, reveals an intracellular "RCK" domain that is similar to portions of Slo's intracellular domain, and this RCK domain forms the bacterial channel's Ca^{2+}-binding "gating ring" (Jiang et al., 2001, 2002). Second, mutations in and around Slo's RCK domain decrease the BK_{Ca} channel's Ca^{2+} sensitivity (Wei et al., 1994; Shi and Cui, 2001; Zhang et al., 2001; Bao et al., 2002; Shi et al., 2002). And third, several experiments suggest that an acidic region in Slo's intracellular domain termed the "Ca^{2+} bowl" may form a Ca^{2+}-binding site: Fairly large mutations in the Ca^{2+} bowl reduce the channel's Ca^{2+} sensitivity by approximately half (Bian et al., 2001; Bao et al., 2002; Xia et al., 2002). When a portion of Slo that includes the Ca^{2+} bowl was transferred to the Ca^{2+}-insensitive Slo3 subunit, Ca^{2+} sensitivity was conferred upon the previously insensitive channel (Schreiber et al., 1999). And peptides composed of por-

Address correspondence to Daniel H. Cox, 750 Washington St., NEMC Hospitals, Box 7868, Boston, MA 02111. Fax: (617) 636-0576; email: dan.cox@tufts.edu

 J. Gen. Physiol. © The Rockefeller University Press • 0022-1295/2004/05/475/15 $8.00
Volume 123 May 2004 475–489
http://www.jgp.org/cgi/doi/10.1085/jgp.200409052

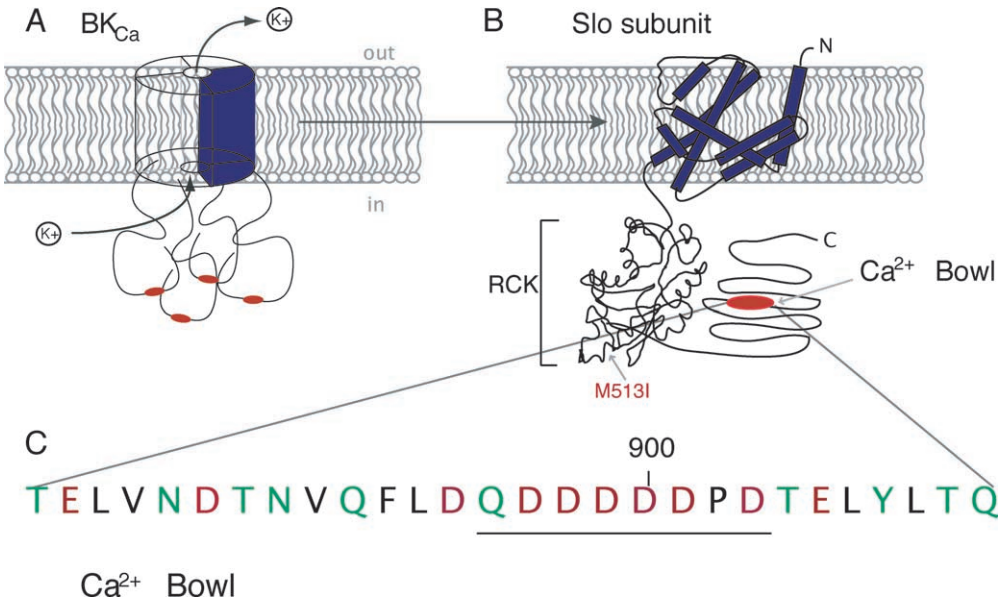

FIGURE 1. General topology of the BK_{Ca} channel. (A) Diagram of the fourfold-symmetric BK_{Ca} channel, composed of four "slo" subunits. (B) Putative topology of a single subunit. Apparent is the integral-membrane domain (based loosely on the recent structure of the KvAP channel; Jiang et al., 2003) and the intracellular domain. In the latter are indicated the RCK domain, whose representation was modeled after the structure of the MthK channel's RCK domain (Jiang et al., 2002), and the Ca^{2+} bowl, whose structure is unknown. (C) Amino acid sequence of the Ca^{2+} bowl. Residues with acidic side chains are indicated in red. Other oxygen-containing side chains are indicated in green. Side chains without oxygen are indicated in black.

tions of Slo that include the Ca^{2+} bowl bind Ca^{2+} in gel-overlay assays (Bian et al., 2001; Braun and Sy, 2001), and this binding is inhibited by the mutation of five Ca^{2+}-bowl aspartic acids (Bian et al., 2001).

Thus, there is evidence both for and against the notion that Ca^{2+} binds to the BK_{Ca} channel's intracellular domain, specifically to the Ca^{2+} bowl, and in general there is a good deal of confusion as to where Ca^{2+} binds to the BK_{Ca} channel and to what degree mutations that affect Ca^{2+}-dependent channel opening are acting at the point of Ca^{2+} coordination. If, however, the Ca^{2+} bowl forms a functionally relevant Ca^{2+}-binding site, then we might make two predictions. First, residues in the Ca^{2+} bowl that coordinate Ca^{2+} should in general be more sensitive to mutation than those that do not directly contact Ca^{2+} (Falke et al., 1994). And second, a correlation should exist between Ca^{2+}-bowl mutations that affect Ca^{2+} sensing and those that affect Ca^{2+} binding. To test these predictions, and to perhaps identify residues involved in Ca^{2+} binding, we made a series of point mutations in the mouse Slo (mSlo) Ca^{2+} bowl and analyzed the effect of each on the energy-change that Ca^{2+} binding imparts to the mSlo channel's closed-to-open conformational change. Also, we have examined, by gel-overlay, the effect of many of these mutations on Ca^{2+} binding to a fusion protein that contains a portion of mSlo's COOH-terminal tail. Our results reveal a subregion of the Ca^{2+} bowl that is critical for both Ca^{2+} sensing and Ca^{2+} binding, and they identify two aspartates in this subregion that are essential for both processes. Thus, much of our data suggests that the Ca^{2+} bowl forms a functionally relevant Ca^{2+}-binding site. Overall, however, we have found that the relationship between mutations that disrupt Ca^{2+} sensing and those that disrupt Ca^{2+} binding is not as strong as we had expected, a result that raises the possibility that, when examined by gel-overlay, the Ca^{2+} bowl may be in a nonnative conformation.

MATERIALS AND METHODS

Channel Expression and Electrophysiology

All electrophysiology experiments were done with the *mslo* clone mbr5 (Butler et al., 1993) essentially as described (Bao et al., 2002). In vitro transcription was performed with the mMessage mMachine kit with T3 RNA polymerase (Ambion). To record macroscopic currents ~0.5–50 ng of cRNA were injected into *Xenopus laevis* oocytes (stage IV-V) 2–6 d before recording.

All recordings were done in the inside-out patch-clamp configuration (Hamill et al., 1981). Patch pipettes were made of borosilicate glass (VWR micropipettes), and had resistances of 1–2 MΩ in our recording solutions. Their tips were coated with sticky wax (Sticky Wax) and fire polished before use. Data were acquired using Axopatch 200B patch-clamp amplifiers (Axon Instruments, Inc.) and Macintosh-based computer systems that use "Pulse" acquisition software (HEKA Electronik) and the ITC-16 hardware interface (Instrutech Scientific Instruments). Records were digitized at 50 Khz and low pass filtered at 10 KHz. All experiments were performed at room temperature, 22–24°C. Before current records were analyzed and displayed, capacity and leak currents were subtracted using a P/5 leak subtraction protocol with a holding potential of −120 mV and voltage steps opposite in polarity to those in the experimental protocol.

Mutagenesis

All mutations were made with the QuickChange site-directed-mutagenesis kit (Stratagene), and mutations were identified by sequencing around the point of the mutation.

Solutions

Recording solutions were composed of the following (in mM): pipette solution, 80 $KMeSO_3$, 60 N-methyl-glucamine-$MeSO_3$, 20 HEPES, 2 KCl, 2 $MgCl_2$, pH 7.20. Internal solution, 80 $KMeSO_3$, 60 N-methyl-glucamine-$MeSO_3$, 20 HEPES, 2 KCl, 1 HEDTA or 1 EGTA, and $CaCl_2$ sufficient to give the appropriate free Ca^{2+} concentration; pH 7.20). EGTA (Sigma-Aldrich) was used as the Ca^{2+} buffer for the 0.003 μM [Ca^{2+}] solutions. HEDTA (Sigma-Aldrich) was used as the Ca^{2+} buffer for solutions containing 0.8 and 10 μM free [Ca^{2+}]. 50 μM (+)-18-crown-6-tetracarboxylic acid (18C6TA) was added to all internal solutions to prevent Ba^{2+} block at high voltages.

The appropriate amount of total Ca^{2+} (100 mM $CaCl_2$ standard solution; Orion Research, Inc.) to add to the base internal solution containing 1 mM HEDTA to yield the desired free Ca^{2+} concentration was calculated using the program Max Chelator (Bers et al., 1994), which was downloaded from (www.stanford.edu/~cpatton/maxc.html), and the proton and Ca^{2+}-binding constants of Bers (supplied with the program) for pH = 7.20, T = 23°C, and ionic strength = 0.15. The ability of 18C6TA to chelate Ca^{2+}, as well as K^+ and Ba^{2+}, was also considered in these calculations using the following dissociation constants: Ca^{2+} 10^{-8} M (Dietrich, 1985), K^+ 3.3×10^{-6} M (Dietrich, 1985), Ba^{2+} 1.6×10^{-10} M (Diaz et al., 1996). Free [Ca^{2+}] was measured with a Ca-sensitive electrode (Orion Research, Inc.), and the measured value reported. Endogenous [Ca^{2+}] in our internal solution before addition of Ca^{2+} chelator was estimated from the deviation from linearity of the Ca-sensitive electrode's response at 10 μM added [Ca^{2+}], and was 16–20 μM. Endogenous [Ca^{2+}] was then compensated for when making Ca^{2+}-buffered solutions. 1 mM EGTA was added to the internal solution intended to contain 0.003 μM free Ca^{2+}, and no Ca^{2+} was added.

During our experiments the solution bathing the cytoplasmic face of the patch was exchanged using a sewer-pipe flow system (DAD 12) purchased from Adams and List Assoc. Ltd.

Data Analysis

G-V relations were determined from the amplitude of tail currents measured 200 μs after repolarization to a fixed membrane potential (−80 mV) after voltage steps to the indicated test voltages. Each G-V relation was fitted with a Boltzmann function ($G = G_{max}/(1 + e^{-zF(V - V1/2)/RT})$) and normalized to the peak of the fit. All curve fitting was done with "Igor Pro" graphing and curve fitting software (WaveMetrics, Inc.) using the Levenberg-Marquardt algorithm to perform nonlinear least squares fits. This software was also used to fit Eq. 2 to the G-V relations of each experiment as described with reference to Fig. 4. The constant parameters used for these fits were as follows: $J_C(0) = 0.059$; $J_O(0) = 1.020$; $z = 0.51$; $q = 0.4$.

To determine the statistical significance of the data in Figs. 4–6, Student's t statistic (difference in sample means/standard error of difference of sample means) was calculated according to Eq. 1 below for either $\Delta V_{1/2}$ or $\Delta\Delta G_{Ca}$ and compared against the t distribution with degrees of freedom: sum of all $n - 4$.

$$t = \frac{\overline{\Delta V}_{1/2_{control}} - \overline{\Delta V}_{1/2_{mutant}}}{\sqrt{\frac{\sigma^2_{Con-3nm}}{n_{Con-3nm}} + \frac{\sigma^2_{Con-10\mu m}}{n_{Con-10\mu m}} + \frac{\sigma^2_{Mut-3nm}}{n_{Mut-3nm}} + \frac{\sigma^2_{Mut-10\mu m}}{n_{Mut-10\mu m}}}}. \quad (1)$$

Expression and Purification of GST-fusion Proteins

An EcoRI-NotI fragment encoding 207 amino acids from the COOH terminus of the mouse Slo (mbr5) subunit ranging from ASNFHY to GATPEL was subcloned in frame with the glutathione-S-transferase (GST) of the bacterial expression plasmid pGEX-4T-1 to make the GST-mSlo207 expression vector. The QuickChange site-directed mutagenesis kit (Stratagene) and standard subcloning techniques were used to create the GST-mSlo207 mutant expression constructs. After transformation into *Escherichia coli* strain BL21, a 6 ml LB/amp (100 μg/ml) overnight culture was used to inoculate 200 ml of LB/amp. The culture was grown for 1.5–2 h ($A_{600} = 0.8$) at 37°C and then induced with isopropylthio-β-galactoside (IPTG) (0.1 mM) for 4 h. Bacterial cells were collected and frozen. Cells were thawed at room temperature and resuspended in 10 ml of ETN washing buffer (20 mM Tris, pH 8.0; 100 mM NaCl; 1.5 mM EDTA; 0.1% sarcosyl; protease inhibitors). Cells were kept on ice for 15 min. Additional EDTA (final concentration is 5–6 mM) and sarcosyl (final concentration is 1.4%) were added. Cells were sonicated on ice and then spun down at 10,000 rpm for 50 min at 4°C. Supernatants were collected and poured into 50-ml tubes, then divided into two tubes. To each fraction, 10 ml of 10% Triton X-100 was added and gently mixed. One fraction was frozen at −80°C. To the other fraction, 500–700 μl of blocked glutathione agarose beads (Sigma-Aldrich) were added and incubated with rocking for 2 h at 4°C. The beads were then washed three times with 10 ml of cold PBS (centrifuge at 1,000 rpm for 2 min, and rock for 5 min at 4°C in between washes). Beads were stored at 4°C in an equal volume of cold PBS with the addition of 50 μl of 2% NaN_2. Protein was eluted from the beads with 1% SDS in PBS, and concentrated with vivaspin ultrafiltration concentrators (Vivascience). Protein concentrations were then measured by Bradford Assay (Bio-Rad Laboratories).

$^{45}Ca^{2+}$-overlay Assays

Ca^{2+} overlay assays were done essentially as described by Braun and Sy (2001). After SDS-PAGE, protein bands—between 10 and 60 μg per lane— were electroblotted onto a nitrocellulose membrane, which was then dried for 30 min at room temperature. The effectiveness of protein transfer was examined by ponceau staining (Sigma-Aldrich). The stain was then removed by washing the blot with PBS, and the blot was washed further at room temperature 4 × 10 min in 30 ml wash buffer (10 mM imidazole-HCl, 70 mM KCl, pH 6.8; this solution was treated with 1 g/l chelex 100 [Bio-Rad Laboratories] to reduce the amount of contaminant Ca^{2+}), after which the membranes were rocked at room temperature in 30-ml wash buffer with 10 μCi/ml added $^{45}CaCl_2$ (ICN) (between 9 and 12 μM) for 1 h. This was followed by a single 5-min wash in 50% ethanol. After the blot was hung dry overnight, it was exposed to a phosphorscreen for 6–7 h. Bands were detected by the PhosphorImager system of Molecular Dynamics, Inc. The relative amounts of $^{45}Ca^{2+}$ binding were quantified using the densitometric software ImageQuant also from Molecular Dynamics, Inc. Due to problems with consistent washing across blots, we were unable to generate Ca^{2+}-binding curves with this assay.

Molecular Modeling

The Ca^{2+}-bowl residues 896–907 where modeled according to the backbone carbon trace of the first Ca^{2+}-binding loop of parvalbumin (PDB entry 2PVB, residues 51–62). Alignment and energy minimization was done with InsightII software (Accelrys, Inc).

The BK_{Ca} channel opens in response to both changes in membrane potential and internal Ca^{2+} concentration ($[Ca^{2+}]$) such that increases in $[Ca^{2+}]$ shift the BK_{Ca} channel's G-V relation leftward along the voltage axis (Fig. 2 A). For a given change in $[Ca^{2+}]$ the magnitude of the shift depends on the three factors: the voltage sensitivity of the channel, the energetics of Ca^{2+} binding, and the number of binding sites that influence opening (Cox et al., 1997). Recent analyses of mSlo mutants have suggested that three types of Ca^{2+}-binding sites influence opening—one of low affinity that starts to affect G-V position at ~10 μM $[Ca^{2+}]$ and two of higher affinity, both of which start to affect G-V position at ~0.1 μM $[Ca^{2+}]$ (Zhang et al., 2001; Bao et al., 2002; Shi et al., 2002; Xia et al., 2002). Given the fourfold symmetry of the channel (Shen et al., 1994), and recent results with hybrid channels (Niu and Magleby, 2002), it seems likely that there are four of each type of binding site.

One type of high-affinity Ca^{2+}-binding site can be functionally disrupted by point mutations in and around the channel's RCK domain (Bao et al., 2002; Xia et al., 2002). Such mutations reduce by approximately half the G-V shift observed in response to micromolar $[Ca^{2+}]$, as expected if these mutations cause the loss of half of the channel's functionally similar, high-affinity Ca^{2+}-binding sites. This is illustrated in Fig. 2 B with the mutant M513I. The second type of high-affinity site can be similarly disrupted by large mutations in the acidic region of the Ca^{2+} bowl (Schreiber and Salkoff, 1997; Bian et al., 2001; Bao et al., 2002; Xia et al., 2002). This is illustrated in Fig. 2 C with the deletion mutant Δ896–903 (Bao et al., 2002). When mutations at both positions are made together, all high-affinity response is lost (Fig. 2 D) (Bao et al., 2002; Xia et al., 2002). This result is important in the present context, because it indicates that the mSlo channel contains no other high-affinity Ca^{2+}-binding sites. Thus, if we want to study the BK_{Ca} channel's Ca^{2+}-bowl–related Ca^{2+}-binding sites in isolation, or more precisely those sites whose functional effects are altered by mutations in the Ca^{2+} bowl, we may do so by working with a channel that carries the M513I mutation. This is the approach we have taken in this study. Also, to prevent interference from the channel's low-affinity sites we have restricted our analysis to Ca^{2+} concentrations less than or equal to 10 μM (Zhang et al., 2001; Bao et al., 2002).

An Alanine Scan of the Ca^{2+} Bowl

Shown in Fig. 1 C is the sequence of the "Ca^{2+} bowl" as delineated by Schreiber and Salkoff (1997). Residues with negatively charged side-chains at neutral pH are indicated in red; other oxygen-containing side chains are shown in green. As Ca^{2+}-binding sites in proteins are universally formed by oxygen atoms—typically six or seven coordinate the Ca^{2+} ion, one or two of which are supplied by water (Falke et al., 1994; Nalefski and Falke, 1996; Perisic et al., 1998)—it seems likely that if the Ca^{2+} bowl forms a Ca^{2+}-binding site, then some of these oxygen-containing side chains are involved. From the Δ896–903 mutant's (plus M513I) complete loss of

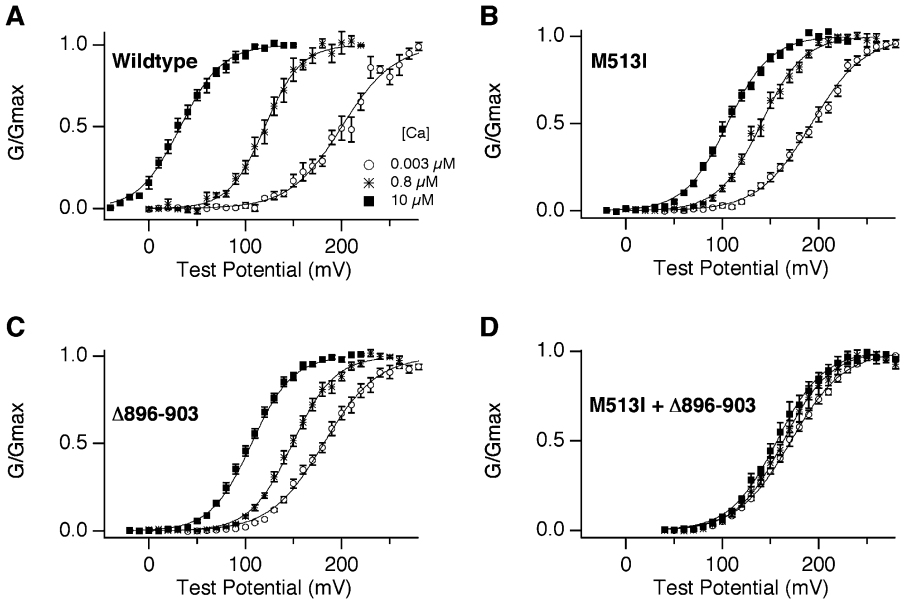

FIGURE 2. mSlo mutations that eliminate high-affinity Ca^{2+} sensing. Average normalized G-V relations determined at 0.003, 0.8, and 10 μM internal $[Ca^{2+}]$. Data are from inside-out *Xenopus* oocyte macropatches expressing cRNA from either (A) wild-type mSlo, (B) the RCK mutant M513I, (C) the Ca^{2+}-bowl deletion mutant Δ896–903, or (D) the double mutant M513I + Δ896–903. Notice each mutation eliminates half of the channel's Ca^{2+}-induced G-V shift. Each G-V curve is fitted with a Boltzmann function whose parameters where as follows. Wild-type: 0.003 μM $[Ca^{2+}]$ $V_{1/2}$ = 200 mV, z = 0.93; 0.8 μM $[Ca^{2+}]$ $V_{1/2}$ = 120 mV, z = 1.36; 10 μM $[Ca^{2+}]$ $V_{1/2}$ = 32.8 mV, z = 1.18. *M513I*: 0.003 μM $[Ca^{2+}]$ $V_{1/2}$ = 193 mV, z = 0.92; 0.8 μM $[Ca^{2+}]$ $V_{1/2}$ = 140 mV, z = 1.16; 10 μM $[Ca^{2+}]$ $V_{1/2}$ = 106 mV, z = 1.14. *Δ896–903*: 0.003 μM $[Ca^{2+}]$ $V_{1/2}$ = 182 mV, z = 0.92; 0.8 μM $[Ca^{2+}]$ $V_{1/2}$ = 149 mV, z = 1.17; 10 μM $[Ca^{2+}]$ $V_{1/2}$ = 105 mV, z = 1.23. *M513I + Δ896–903*: 0.003 μM $[Ca^{2+}]$ $V_{1/2}$ = 172 mV, z = 0.93; 0.8 μM $[Ca^{2+}]$ $V_{1/2}$ = 164 mV, z = 1.05; 10 μM $[Ca^{2+}]$ $V_{1/2}$ = 157 mV, z = 1.05. These data have been discussed previously in Bao et al. (2002). Error bars here and elsewhere indicate standard error of the mean.

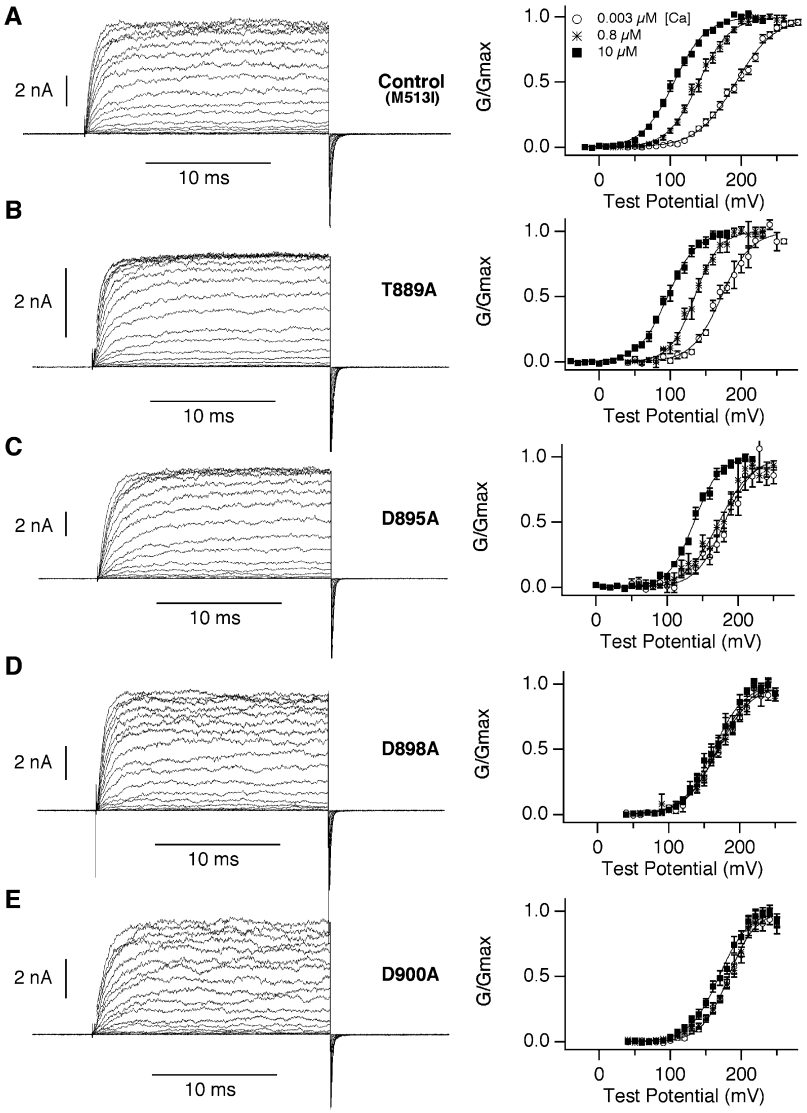

FIGURE 3. Three classes of Ca^{2+}-bowl point mutants. Shown are data from (A) our control (M513I) channel, (B) a mutant that showed little change in Ca^{2+} response, (C) a mutant whose Ca^{2+} response was reduced by approximately half, and (D and E) two mutants whose responses to 10 μM $[Ca^{2+}]$ were essentially eliminated. On the left are current families (10 μM $[Ca^{2+}]$) representative of those used to generate the G-V curves on the right. Voltages are as follows. Control (M513I): hold −50 mV, test 0–180 mV. T889A: hold −80 mV, test 0–180 mV. D895A: hold −50 mV, test 0–200 mV. D898A: hold −50 mV, test 40–220 mV. D900A: hold −50 mV, test 40–230 mV. All repolarization were to −80 mV. G-V Boltzmann fit parameters where as follows. Control: as in the legend to Fig. 2. *T899A*: 0.003 μM $[Ca^{2+}]$ $V_{1/2}$ = 172 mV, z = 1.21; 0.8 μM $[Ca^{2+}]$ $V_{1/2}$ = 135 mV, z = 1.46; 10 μM $[Ca^{2+}]$ $V_{1/2}$ = 96 mV, z = 1.24. *D895A*: 0.003 μM $[Ca^{2+}]$ $V_{1/2}$ = 181 mV, z = 1.24; 0.8 μM $[Ca^{2+}]$ $V_{1/2}$ = 173 mV, z = 1.08; 10 μM $[Ca^{2+}]$ $V_{1/2}$ = 138 mV, z = 1.42. *D898A*: 0.003 μM $[Ca^{2+}]$ $V_{1/2}$ = 170 mV, z = 1.06; 0.8 μM $[Ca^{2+}]$ $V_{1/2}$ = 169 mV, z = 1.14; 0.8 μM; 10 μM $[Ca^{2+}]$ $V_{1/2}$ = 163 mV, z = 1.17. *D900A*: 0.003 μM $[Ca^{2+}]$ $V_{1/2}$ = 182 mV, z = 1.34; 0.8 μM $[Ca^{2+}]$ $V_{1/2}$ = 182 mV, z = 1.33; 10 μM $[Ca^{2+}]$ $V_{1/2}$ = 169 mV, z = 1.22.

Ca^{2+} sensitivity (Fig. 2 D) we know that one or more of the eight amino acids deleted in this mutant (underlined in Fig. 1 C) are critical for Ca^{2+}-bowl function. Seven of these residues contain side-chain oxygens and six of them are acidic. Similar results have been obtained for the smaller deletion mutant Δ899–903 (Bao et al., 2002) and for the substitution mutant 897–901N (Xia et al., 2002). The structures of residues D899, D900, and D901 or some subset of these, therefore, must be important for proper Ca^{2+} sensing. Effects on Ca^{2+} sensing have also been reported, however, for mutations at D897 and D898 (Schreiber and Salkoff, 1997), so perhaps these residues are important as well, and clearly, as the great majority have not been tested, there could be many other residues in the Ca^{2+}-bowl whose side-chains are also involved in Ca^{2+} sensing.

To examine each residue individually, we mutated each oxygen-containing side-chain in the Ca^{2+} bowl (each red or green residue in Fig. 1 C) to alanine, one at a time, and looked for effects on Ca^{2+}-sensing. As shown in Fig. 3, three general phenotypes were observed. Most mutants (e.g., T889A, Fig. 3 B) showed little or no change in Ca^{2+} response. This was the case for 11 of the 20 mutants tested. Nine mutants showed reduced Ca^{2+}-sensitivity, as judged by a decrease in G-V-shift in response to micromolar $[Ca^{2+}]$. An example of one such mutant, D895A, whose G-V shift in response to 10 μM $[Ca^{2+}]$ is reduced by approximately half, is shown in Fig. 3 C. Most interesting, however, were two mutants, D898A and D900A (Fig. 3, D and E); each exhibited essentially no response to 10 μM $[Ca^{2+}]$. Thus, large deletions or substitutions are not required to eliminate Ca^{2+} sensing via the Ca^{2+}-bowl–related site; a single-point mutation at D898 or D900 is sufficient.

These results are summarized in Fig. 4 A, where we have plotted for each mutant tested the change in half-maximal activation voltage ($\Delta V_{1/2}$) observed in response to increasing $[Ca^{2+}]$ from 0.003 to 10 μM.

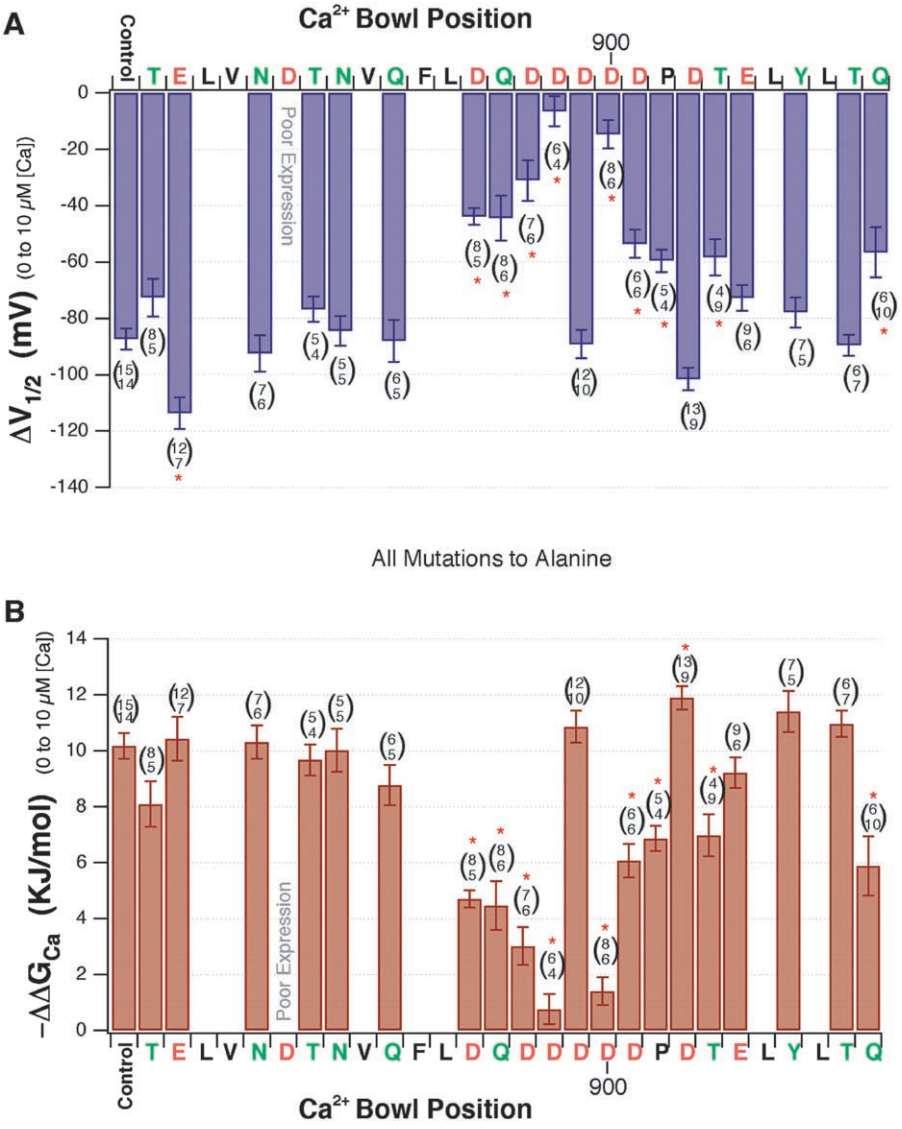

FIGURE 4. Summary of the effects of point mutations in the Ca^{2+} bowl. (A) Change in average $V_{1/2}$ in response to increasing $[Ca^{2+}]$ from 0.003 to 10 μM for each of a series of point mutations to alanine in the Ca^{2+} bowl. Each mutated amino acid and its position in the Ca^{2+} bowl is indicated along the horizontal axis. Residues with acidic side-chains are indicated in red. Other oxygen-containing side chains are indicated in green. Side-chains without oxygen are indicated in black. Mutant responses that are statistically significant relative to control (far left) are indicated with an asterisk. The number of measurements (n) for each data point is indicated in parentheses with the upper number indicating n for 10 μM and the lower number indicating n for 0.003 μM $[Ca^{2+}]$. (B) Effect of raising $[Ca^{2+}]$ from 0.003 to 10 μM on the free-energy difference between open and closed. $-\Delta\Delta G_{Ca}$ (0.003–10 μM $[Ca^{2+}]$) values were determined from G-V fits to Eq. 2 as described in the text. The following constant parameters were used: $J_C(0) = 0.059$; $J_O(0) = 1.020$; $z = 0.51$; $q = 0.4$. The dataset used in B is the same as in A.

When the data are viewed in this way, a trend becomes apparent. The most effective mutations involve the very acidic region between D895 and D903 with a rough progression as one moves from the center of this region toward either end. D898A and D900A are most effective, and then D897A, Q896A, and D895A are less so on the left, and similarly D901A and P902A are less so on the right. What is striking, however, is that D899A, a substitution at the very center of this acidic region, and one flanked by D898 and D900, is without effect.

To convert these results into energetic terms (Bao et al., 2002) we used a model of the BK_{Ca} channel's voltage-dependent gating mechanism developed by Horrigan and Aldrich (1999). G-V curves from each experiment were fitted with Eq. 2, which describes the open probability of the Horrigan and Aldrich (1999) model as a function of voltage (V).

$$P_{open} = \frac{1}{1 + \left[\frac{1 + J_C(0)\,e^{zFV/RT}}{1 + J_O(0)\,e^{zFV/RT}}\right]^4 A_{Ca}\,e^{-qFV/RT}}. \qquad (2)$$

Here $J_O(0)$ and $J_C(0)$ represent the equilibrium constants for voltage-sensor movement in each subunit at 0 mV when the channel is open or closed, respectively, z represents the gating charge associated with each voltage sensor, q represents the gating charge associated with the model channel's central conformational change, and (most pertinent here) A_{Ca} represents a Ca^{2+}-dependent factor that is logarithmically related to the free energy difference between open and closed at 0 mV as follows:

$$\Delta G(0)_{O-C} = 4RT\ln\left[\frac{1 + J_C(0)}{1 + J_O(0)}\right] + RT\ln[A_{Ca}]. \qquad (3)$$

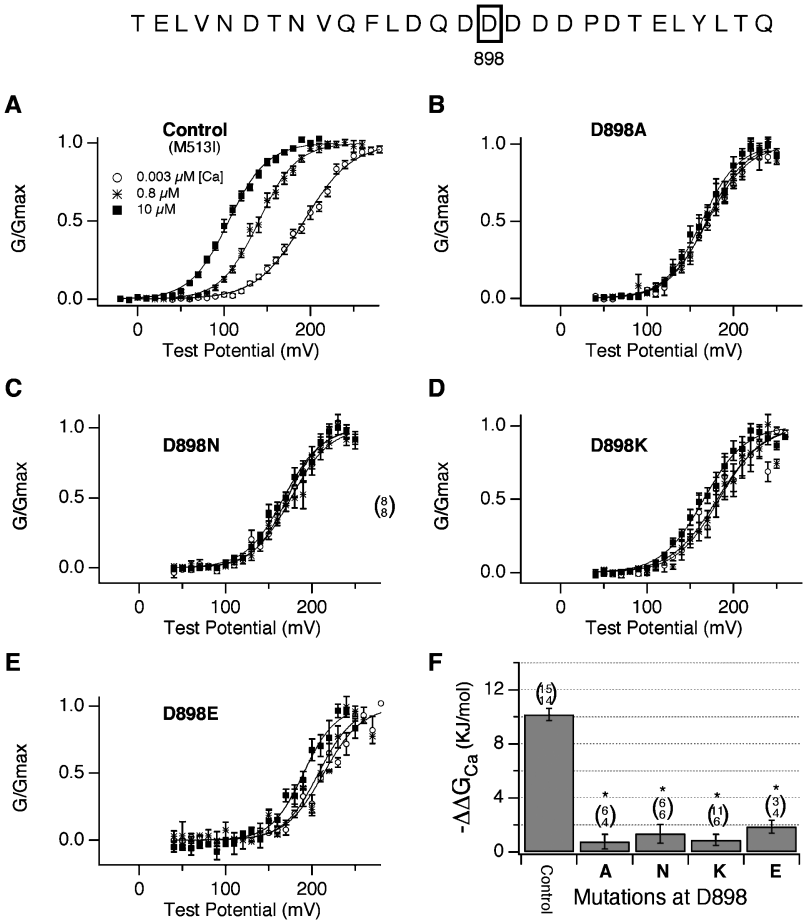

FIGURE 5. Ca^{2+} sensing is very sensitive to the nature of the residue at position 898. G-V curves determined for (A) the control (M513I) channel, and (B–E) four mutations at position 898 as indicated. (F) The effect of raising $[Ca^{2+}]$ from 0.003 μM to 10 μM on the free-energy difference between open and closed. $-\Delta\Delta G_{Ca}$ (0.003–10 μM $[Ca^{2+}]$) values were determined as described in the text. Control: as in the legend to Fig. 2. *D898A*: as in the legend to Fig. 3. *D898N*: 0.003 μM $[Ca^{2+}]$ $V_{1/2}$ = 172 mV, z = 1.28; 0.8 μM $[Ca^{2+}]$ $V_{1/2}$ = 176 mV, z = 1.15; 10 μM $[Ca^{2+}]$ $V_{1/2}$ = 168 mV, z = 1.16. *D898K*: 0.003 μM $[Ca^{2+}]$ $V_{1/2}$ = 181 mV, z = 0.95; 0.8 μM $[Ca^{2+}]$ $V_{1/2}$ = 184 mV, z = 1.02; 10 μM $[Ca^{2+}]$ $V_{1/2}$ = 166 mV, z = 1.05. *D898E*: 0.003 μM $[Ca^{2+}]$ $V_{1/2}$ = 214 mV, z = 1.15; 0.8 μM $[Ca^{2+}]$ $V_{1/2}$ = 208 mV, z = 1.25; 10 μM $[Ca^{2+}]$ $V_{1/2}$ = 191 mV, z = 1.35.

Thus, from A_{Ca}, $J_C(0)$, and $J_O(0)$ we can estimate $\Delta G(0)_{O-C}$ as a function of $[Ca^{2+}]$ for each mutant and then subtract to calculate $\Delta\Delta G_{Ca}$(0.003–10 μM), the change in this free-energy difference as $[Ca^{2+}]$ is raised from 0.003 (nominally 0) to 10 μM. In so doing we constrained the fitting by using voltage-dependent gating parameters close to those determined for mSlo by Horrigan et al. (1999) (see also Cox and Aldrich, 2000), which is equivalent to assuming that Ca^{2+}-bowl mutations do not affect voltage-sensor movement directly. This is perhaps a questionable assumption, but one we think is reasonable, given that Ca^{2+} binding and voltage-sensor movement affect channel opening independently (Cox et al., 1997; Cui and Aldrich, 2000; Rothberg and Magleby, 2000; Horrigan and Aldrich, 2002), and that, in general, we have observed little effect of each Ca^{2+}-bowl mutation on the mSlo channel's G-V relation in the absence of $[Ca^{2+}]$ (for examples see Fig. 3). The results of this analysis are shown in Fig. 4 B, and, as is evident, they are qualitatively similar to those observed for $\Delta V_{1/2}$. The side chains of D898 and D900 are critical for Ca^{2+} sensing, and mutations around this region, except for D899A, reduce $\Delta\Delta G_{Ca}$ by a third to two thirds.

Aspartates Are Needed at 898 and 900 for Ca^{2+} Sensing

Thus, effective mutations in the Ca^{2+} bowl lie in a cluster that might reasonably form a Ca^{2+}-binding site, and if this is the case, then carboxylate oxygens from residues D898 and D900 are likely to be required for Ca^{2+} coordination. To test this hypothesis we mutated D898 and D900 one at time to asparagines, thereby substituting in each case a neutral amide for a similarly sized carboxylate. Despite the minimal nature of these mutations, however, as is consistent with our hypothesis, they also eliminated Ca^{2+}-bowl function (Fig. 5 C and Fig. 6 C). In addition, we obtained similar results when each of these residues was mutated individually to a positively charged lysine (Figs. 5 D and 6 D). Thus, the negatively-charged carboxylate oxygen's of D898 and D900 are essential for Ca^{2+}-bowl function. When we mutated D898 or D900 to glutamate, however, maintaining the negative charge, Ca^{2+} sensitivity was also largely lost (Figs. 5 E and 6 E). The mutant channels were in each case slightly more responsive to Ca^{2+} than the corresponding aspartate-to-alanine mutant, but not to a statistically significant degree and much less so than was the control M513I channel. Thus, at either position

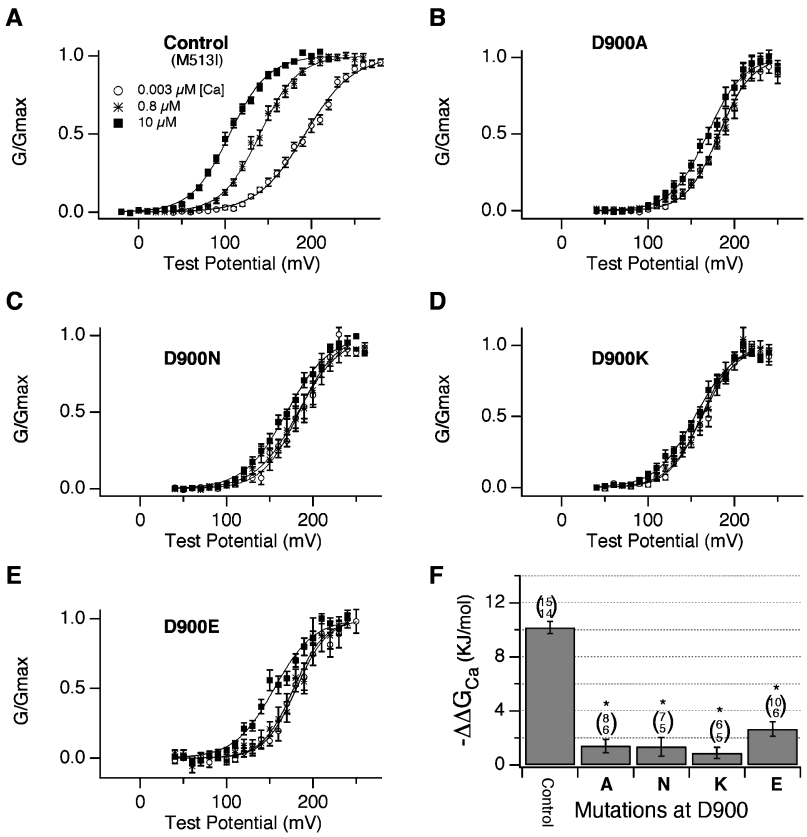

FIGURE 6. Ca^{2+} sensing is very sensitive to the nature of the residue at position 900. G-V curves determined for (A) the control (M513I) channel, and (B–E) four mutations at position 900 as indicated. (F) The effect of raising $[Ca^{2+}]$ from 0.003 to 10 μM on the free-energy difference between open and closed. $-\Delta\Delta G_{Ca}$ (0.003–10 μM $[Ca^{2+}]$) values were determined as described in the text. Control as in the legend to Fig. 2. *D900A*: as in the legend to Fig. 3. *D900N*: 0.003 μM $[Ca^{2+}]$ $V_{1/2}$ = 184 mV, z = 1.20; 0.8 μM $[Ca^{2+}]$ $V_{1/2}$ = 183 mV, z = 1.04; 10 μM $[Ca^{2+}]$ $V_{1/2}$ = 170 mV, z = 1.03. *D900K*: 0.003 μM $[Ca^{2+}]$ $V_{1/2}$ = 163 mV, z = 1.26; 0.8 μM $[Ca^{2+}]$ $V_{1/2}$ = 162 mV, z = 1.38; 10 μM $[Ca^{2+}]$ $V_{1/2}$ = 154 mV, z = 1.13. *D900E*: 0.003 μM $[Ca^{2+}]$ $V_{1/2}$ = 181 mV, z = 1.39; 0.8 μM $[Ca^{2+}]$ $V_{1/2}$ = 178 mV, z = 1.39; 10 μM $[Ca^{2+}]$ $V_{1/2}$ = 155 mV, z = 1.10.

glutamate's extra methylene group (as compared with aspartate) is sufficient to disturb Ca^{2+}-bowl function. Charge, therefore, is not the only determinant of function at these residues, and in general it appears that Ca^{2+}-dependent channel opening is very sensitive to changes in structure at residues 898 and 900. Interestingly, if the Ca^{2+} bowl forms a Ca^{2+} binding site, this degree of structural sensitivity at points of Ca^{2+} coordination is not unexpected. In the EF hand–type Ca^{2+}-binding site of troponin C, for example, D–E mutations at either the X or the Y coordinating position reduce the protein's dissociation constant for Ca^{2+} by 10-fold or more, and each mutation also eliminates Ca^{2+}-induced muscle-fiber responses (Babu et al., 1992, 1993).

D898 and D900 Are also Critical for Ca^{2+} Binding

Although the experiments described above indicate that residues in the Ca^{2+} bowl are important for Ca^{2+} sensing, they do not speak directly to the issue of whether or not Ca^{2+} binds to the channel's intracellular domain in general, or the Ca^{2+} bowl in particular. One could imagine that mutations in the Ca^{2+} bowl affect a Ca^{2+}-binding site that resides a considerable distance away, perhaps in the integral-membrane domain. Thus, we employed—as others have done—a $^{45}Ca^{2+}$ gel-overlay assay (Ngai et al., 1987; Bian et al., 2001; Braun and Sy, 2001) to look more directly at Ca^{2+} binding to the channel's intracellular domain. A fusion protein composed of glutathione-*s*-transferase and a 207–amino acid portion of mSlo's intracellular domain—a region that spans from 137 amino acids upstream to 42 amino acids downstream of the Ca^{2+} bowl (Braun and Sy, 2001)—was expressed in, and purified from, bacteria. It was then electrophoresed on a SDS polyacrylamide gel, blotted to nitrocellulose, and exposed to $^{45}Ca^{2+}$. As shown in Fig. 7 A, this fusion protein binds $^{45}Ca^{2+}$, and binding increases as more protein is loaded onto the gel—this blot was exposed to 12 μM $^{45}Ca^{2+}$. Furthermore, binding is greatly attenuated when D898 and D900 are both mutated to alanine (Fig. 7 B). In fact, densitometric measurements of the bands in Fig. 7 B (lower panel) indicate that Ca^{2+} binding is inhibited by 70% when comparing the signal from 10 μg of mutant to 10 μg of wild-type protein, and 86% when comparing 20 μg of each protein. In 32 other experiments very similar results were obtained; on average Ca^{2+} binding was reduced by these mutations by 80 ± 2% (n = 33, SEM). Thus, Ca^{2+} sensing via a site that is

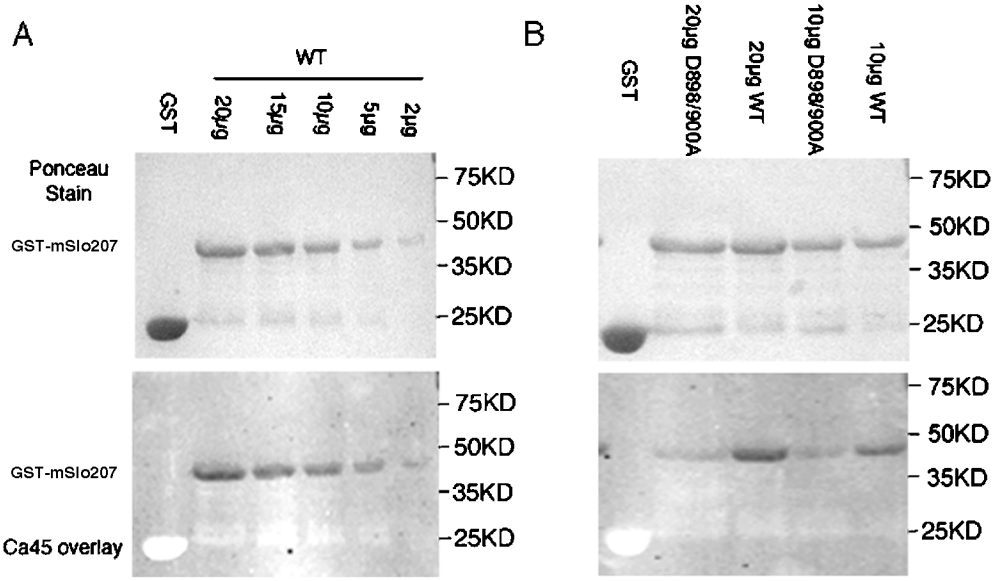

FIGURE 7. Ca^{2+} bowl mutations greatly reduce Ca^{2+} binding to a mSlo fusion protein. (A, top) Ponceau-stained electroblot from and SDS-PAGE gel showing an increasing amount of loaded GST-mSlo207 fusion protein. On the far left 16 µg of GST alone was loaded as a negative control. (A, bottom) Autoradiogram of the blot in the top panel after $^{45}Ca^{2+}$ overlay and wash. Note the increasing signal with increasing protein concentration. (B, top) Ponceau-stained blot from a gel that had loaded onto it 10 and 20 µg of GST-mSlo207 and the mutant GST-mSlo207-D898A/D900A as indicated. On the far left 16 µg of GST alone was loaded as a negative control. (B, bottom) Autoradiogram of the blot in the top panel after over lay with 12 µM $^{45}Ca^{2+}$ and wash.

functionally linked to the Ca^{2+} bowl, and Ca^{2+} binding to a portion of the BK_{Ca} channel's intracellular domain that includes the Ca^{2+} bowl, are both strictly dependent on the structures of the aspartates at positions 898 and 900.

Ca^{2+} Binding to Other Mutant Fusion Proteins

To further explore the correlation between Ca^{2+} binding and Ca^{2+} sensing, we made a series of other mutations in our mSlo-tail fusion protein and examined each of these as well for Ca^{2+} binding, again by gel-overlay. On each gel we ran the wild-type fusion protein and the D898/D900 mutant as positive and negative controls, respectively. Results of these experiments are summarized in Fig. 8 A, where each bar indicates band density as a percentage of wild-type (bar 1, far left). 10 mutations were examined. Results from a number of them correlated well with our electrophysiological data. Mutations E884A and E905A, for example, each of which showed no significant effect on Ca^{2+} sensing (see Fig. 4), also showed no clear effect on Ca^{2+} binding (Fig. 8 A compare bars 2 and 11 to bar 1). Similarly, D903A (bar 10) showed only a small effect on Ca^{2+} binding and no effect electrophysiologically. Furthermore, the double mutant D898E/D900E (bar 8), although it conserves the negative charges of these residues, showed substantial effect on binding, reducing band density by an average of 57 ± 7.5% (n = 4, SEM), and, as discussed above (see Figs. 5 and 6), aspartate-to-glutamate mutations at these positions also showed large effects on Ca^{2+} sensing.

Some of our gel-overlay results, however, were not as consistent with our electrophysiological data. While in our electrophysiological experiments the point mutations D898A and D900A each eliminated Ca^{2+} sensing, these mutations only partially eliminated Ca^{2+} binding (Fig. 8 A, bars 4 and 6; see also Fig. 9), and they were less effective than the double mutation D898A/D900A. Furthermore, D899A, which had no effect on Ca^{2+} sensing, inhibited Ca^{2+} binding by an amount similar to the mutations that eliminated Ca^{2+} sensing, D898A and D900A (Fig. 8 A, bar 5, and Fig. 9, lane 5). Also, the double mutation D899A/D901A was almost as effective at inhibiting Ca^{2+} binding as was D898A/D900A (Fig. 8 A, compare bars 9 and 7), even though the latter was composed of mutations that were each more effective in our electrophysiological experiments than the mutations included in the former. Thus, overall, the correlation between mutations that disrupt Ca^{2+} sensing and those that disrupt Ca^{2+} binding is not as strong as it first appeared.

Why do the mutations D898A and D900A reduce Ca^{2+} binding (on a percentage of wild-type basis) less than they reduce Ca^{2+} sensing? The answer to this question is unclear, however, recalling that Ca^{2+} sensing necessarily depends on there being a difference in affinity between open and closed, we might explain these results by supposing that each single mutation is sufficient to prevent a change in affinity from occur-

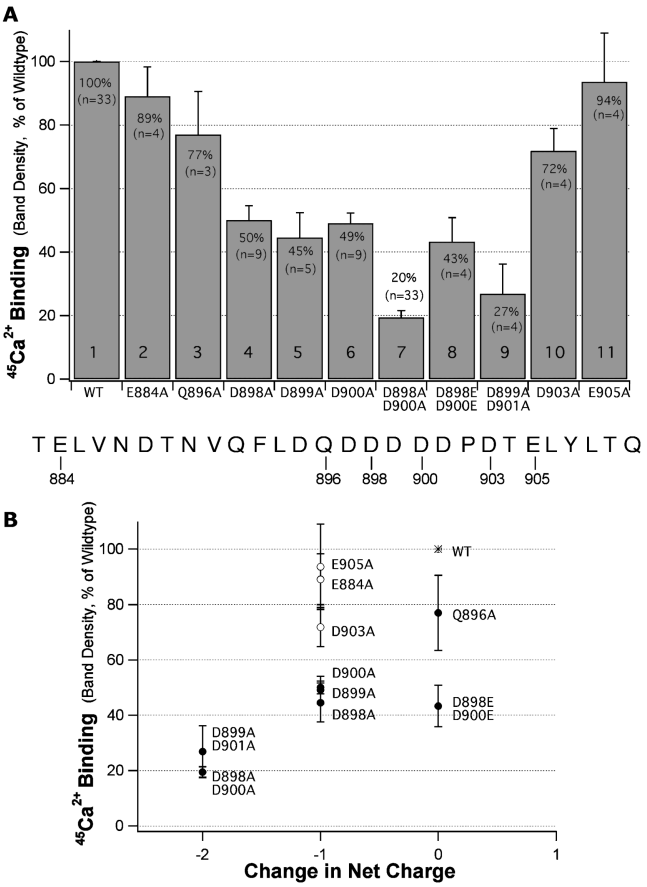

FIGURE 8. Ca^{2+} binding for a series of mutant fusion proteins. (A) $^{45}Ca^{2+}$-band densities from overlay assays are plotted as a percentage of wild-type band density for each of ten GST-mSlo207 fusion proteins. (B) $^{45}Ca^{2+}$-band density is plotted for each mutant fusion protein as a function of the change in net charge each mutation brings about. Open circles indicate mutations outside the central acidic region of the Ca^{2+} bowl (896–901). Closed circles indicate mutations inside this central region.

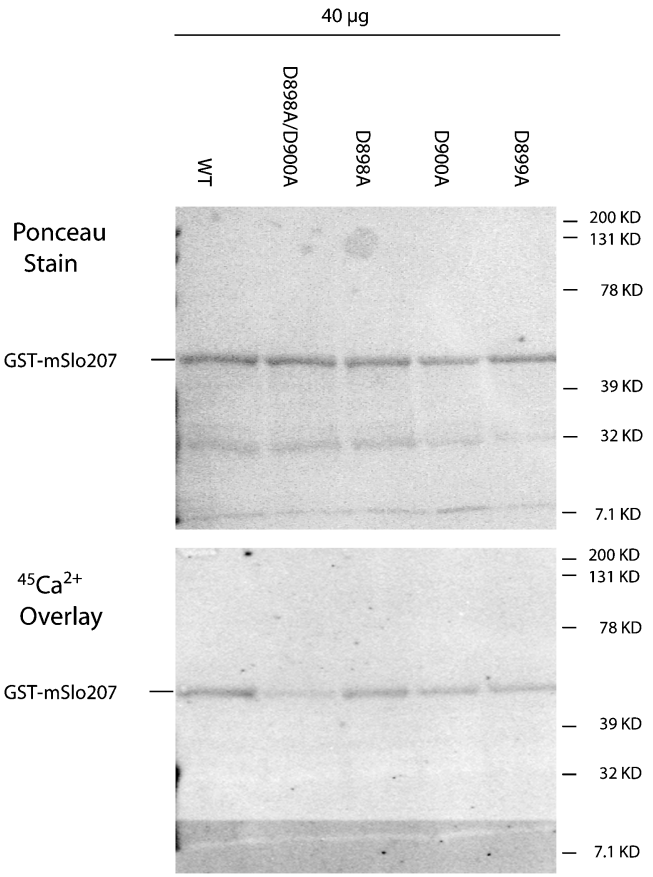

FIGURE 9. Ca^{2+} binding to four Ca^{2+}-bowl mutant fusion proteins. (Top) Ponceau-stained blot from a gel that had loaded onto it 40 µg of GST-mSlo207 and the mutants GST-mSlo207-D898A/D900A, GST-mSlo207-D898A, GST-mSlo207-D900A, and GST-mSlo207-D899A as indicated. (Bottom) Autoradiogram of the blot in the top panel after $^{45}Ca^{2+}$ overlay (9.1 µM [Ca^{2+}]) and wash.

ring as the channel opens at the Ca^{2+}-bowl–related Ca^{2+}-binding site, while both mutations together have a larger effect on the absolute affinity of the site. For example, we have estimated previously that the Ca^{2+}-bowl–related Ca^{2+} binding site has an affinity for Ca^{2+} of ~3.5 µM when the channel is closed and ~0.8 µM when the channel is open (Bao et al., 2002). We do not know whether the Ca^{2+}-bowl–related Ca^{2+}-binding site adopts its open or closed configuration in our fusion protein, but let us suppose it adopts its open, high-affinity configuration. Then, if D898A or D900A raise the dissociation constant of the open configuration (K_O) from 0.8 to 3.5 µM without altering the affinity of the closed configuration (K_C), this would eliminate Ca^{2+} sensing in the intact channel, but it would reduce Ca^{2+} binding to the fusion protein, when exposed to 10 µM [Ca^{2+}], by only a modest 20%. Thus, that some mutations affect Ca^{2+} sensing more than Ca^{2+} binding (in terms of a percentage of maximal $\Delta\Delta G_{Ca}$ and $^{45}Ca^{2+}$-band density), is not altogether unexpected.

The Ca^{2+} Bowl May be Distorted in the Gel Overlay Assay

It is harder, however, to account for the effect of the mutation D899A on Ca^{2+} binding (Fig. 8 A, bar 5). This mutation had no effect on Ca^{2+} sensing (see Fig. 4), but it decreased Ca^{2+} binding by an amount (55 ± 7.8) similar to that observed with the D898A and D900A mutations. According to allosteric theory, in order for D899A to have no effect on Ca^{2+}'s power to shift the mSlo G-V curve, it must not change the channel's Ca^{2+} dissociation-constant ratio K_{Closed}/K_{Open}. However, in order to have some effect in the binding assay it must change at least one of these dissociation constants (the one that corresponds to the binding site's conformation in our fusion protein). Thus, to explain the effects of D899A in both assays we seemingly must suppose that this mutation reduces both K_{Closed} and K_{Open} by a

common factor such that the ratio K_{Closed}/K_{Open} remains unchanged, but Ca^{2+} binding to the fusion protein, when exposed to 10 μM $^{45}Ca^{2+}$, is reduced, because of the now lower affinity of the mutated site.

While the above explanation is not unreasonable, it relies on the idea that D899A reduces K_{Open} and K_{Closed} by a common factor, an occurrence without any obvious physical origin. A more straightforward hypothesis is that Ca^{2+} binds to the fusion protein's Ca^{2+} bowl, but the Ca^{2+} bowl is not in a form that it normally takes in the intact channel. The Ca^{2+} bowl may be in some partially denatured or distorted form such that the determinants of binding are not precisely the same as they are in the intact channel. In fact, viewing the data in Fig. 8 A in this light, it appears that, if we restrict our attention to the region between residues Q896 and D901 inclusive, $^{45}Ca^{2+}$ binding correlates fairly well simply with the charge of this region. This is illustrated by the filled circles in Fig. 8 B, where $^{45}Ca^{2+}$-band density (as a percentage of wild-type) is plotted versus the change in net charge each mutation brings about. Open circles indicate Ca^{2+}-bowl mutations made outside this region, where a change in charge has less effect on binding.

DISCUSSION

An interesting aspect of the gating behavior of the BK_{Ca} channel is the apparent novelty of its Ca^{2+}-sensing mechanism. The channel's pore-forming Slo subunit contains no EF hand, no clear C2 domain, and no other motif that can be described as canonical for Ca^{2+} binding. Yet the channel opens in response to as little as a few hundred nanomolar Ca^{2+}, depending on the membrane potential, so at least moderately high-affinity Ca^{2+}-binding sites must be involved. Indeed, for several years now an acidic region termed the "Ca^{2+} bowl", in the latter part of the channel's intracellular domain, has been implicated in Ca^{2+} sensing (Schreiber and Salkoff, 1997; Schreiber et al., 1999; Bian et al., 2001), and more recently a picture has emerged that suggests that the BK_{Ca} channel contains two types of high-affinity Ca^{2+}-binding sites, both of which reside in the channel's intracellular domain, and one of which is functionally linked to the Ca^{2+} bowl (Schreiber and Salkoff, 1997; Bian et al., 2001; Bao et al., 2002; Xia et al., 2002).

Some Acidic Side Chains Are More Important than Others

Here we have presented a systematic analysis of residues in the Ca^{2+} bowl that are important for Ca^{2+} sensing. And if the Ca^{2+} bowl forms a Ca^{2+}-binding site, then what we have found might be considered not unexpected. The acidic region in the center of the Ca^{2+} bowl (residues 895–903) is most important for Ca^{2+} sensing, and outside of this region, with the exception of Q910, our mutations had little effect. Thus, the side-chain of E884, although acidic, is not required for normal Ca^{2+} sensing, and neither are those of the eight other oxygen-containing side chains outside of this subregion—again, except for Q910. (Note that the mutation at D888 did not express well, so the importance of this residue's side chain is unclear.)

Within the acidic center of the Ca^{2+} bowl, however, all positions do not contribute equally. Single-point mutations of any sort at either D898 or D900 eliminate Ca^{2+} sensing via the Ca^{2+}-bowl–related site, whereas mutations at many other residues in this region—including three aspartates, a glutamine, a proline, and a threonine—show moderate effects. And mutations at the acidic residues D899 and D903 are without effect. Thus, one might speculate that if the Ca^{2+} bowl forms a Ca^{2+}-binding site, then it is the side chains of D898 and D900 that most closely coordinate Ca^{2+} and that many neighboring residues play a lesser role; that is, they may be involved in attracting Ca^{2+} to the site, maintaining the general structure of the region, and/or also providing coordinating ligands. In fact, the observation that the mutations D898A and D900A each eliminate Ca^{2+} sensing, while D899A has no effect, suggests that the Ca^{2+} bowl may form a binding loop with D899 at the center of the turn, its side chain extending away from the Ca^{2+} ion, and D898 and D900, on either side, extending their side chains inward to coordinate Ca^{2+}.

Although clearly speculative, to test the feasibility of this hypothesis we positioned the residues of the acidic region of the Ca^{2+} bowl (residues 896–907) according to the backbone structure of the Ca^{2+} binding loop of parvalbumin (residues 51–62), and then energy minimized this configuration. Interestingly, as shown in Fig. 10, the result of this exercise indicates that such an arrangement is possible, and further, it suggests that the backbone carbonyl oxygen of P902 may also play a role in Ca^{2+} coordination.

Ca^{2+} Binds to the Intracellular Domain

Of course Ca^{2+} sensing and Ca^{2+} binding, although intertwined, are not equivalent. Because Ca^{2+}-dependent channel opening depends on a difference in affinity between open and closed, mutations that eliminate opening in response to Ca^{2+} binding need not destroy binding altogether. And if a mutation eliminates a Ca^{2+}-binding site, it need not sit at the point of Ca^{2+} coordination. Thus, our electrophysiological data are suggestive, but they do not force the conclusion that the Ca^{2+} bowl forms a Ca^{2+}-binding site. Indeed, given recent results that suggest that the BK_{Ca} channel retains its Ca^{2+} sensitivity even after its entire intracellular domain is eliminated (Piskorowski and Aldrich, 2002), indirect effects of mutations at the Ca^{2+} bowl seem an important consideration.

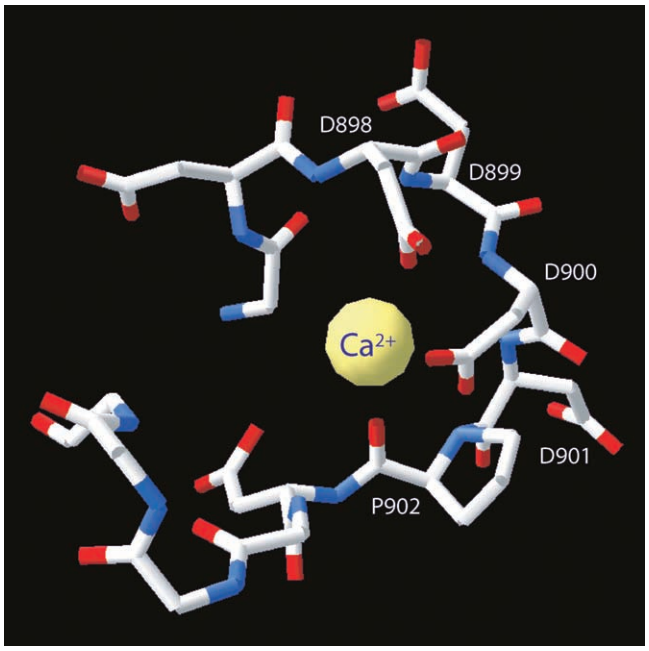

FIGURE 10. Hypothetical model of the Ca^{2+} bowl. Residues 896–907 of mSlo's Ca^{2+} bowl were positioned according to the backbone carbon trace of parvalbumin's first Ca^{2+}-binding loop and energy minimized.

To more directly test for Ca^{2+} binding to the Ca^{2+} bowl we examined, by $^{45}Ca^{2+}$ gel-overlay, Ca^{2+} binding to a series of wild-type and mutant fusion proteins consisting of GST and a portion of the Slo's COOH-terminal "tail" that includes the Ca^{2+} bowl. Most interesting, we found that these fusion proteins do bind Ca^{2+} in this assay, and, just as with Ca^{2+} sensing, it is in the acidic central region of the Ca^{2+} bowl that mutations have greatest influence on Ca^{2+} binding. Furthermore, when we mutated the residues that most effectively disrupted Ca^{2+} sensing, D898 and D900, together to alanine, we saw an 80% decrease in Ca^{2+} binding. Thus, there is a Ca^{2+} binding site within the intracellular region contained in the fusion protein we have used in our binding studies, and it seems likely that this binding site is formed by the Ca^{2+} bowl and relevant to Ca^{2+}-dependent channel opening.

The Ca^{2+} Bowl May be Distorted in Gel-overlay

When we looked more extensively, however, at the relationship between mutations that affect Ca^{2+} sensing and those that affect Ca^{2+} binding, inconsistencies arose that suggest that the structure of the Ca^{2+} bowl in our gel-overlay assay may not be the same as it is in either the open or closed conformation of the intact channel. Most difficult to explain, we found that the mutation D899A had no effect on Ca^{2+} sensing, but it reduced Ca^{2+} binding by an amount similar to D898A and D900A, both of which eliminated Ca^{2+} sensing. And similarly, the double mutant D899A/D901A was almost as effective at reducing Ca^{2+} binding as was the double mutant D898A/D900A, even though the former was composed of two mutations that showed either no or only a partial effect on Ca^{2+} sensing, while the latter was composed of mutations that each eliminated Ca^{2+} sensing. In fact, taken together, our gel-overlay results suggest that in the middle of the Ca^{2+} bowl (895–901), the effects of mutations on Ca^{2+} sensing correlate better with the loss of negatively charged side chains than with the mutation of particular side-chains. Thus, it may be that in our gel-overlay assay the Ca^{2+} bowl takes a conformation that is different from any of its native conformations, one perhaps in which the central Ca^{2+}-bowl aspartates contribute more equally to Ca^{2+} coordination. Considering that during the gel-overlay assay the protein is denatured in the gel and then renatured on the blot, this is perhaps not a surprising conclusion—although this assay has been used successfully with a great many Ca^{2+}-binding proteins, including those with EF hand, C2, and novel types of Ca^{2+}-binding sites (Maruyama et al., 1984; Sienaert et al., 1997; Menguy et al., 1998; Hammarberg et al., 2000; Jegerschold et al., 2000; Rajini et al., 2001; Tompa et al., 2001; Bandyopadhyay et al., 2002; Morohashi et al., 2002). Still, clearly, a different Ca^{2+}-binding assay would be desirable. At present, however, we and others have been limited in this regard by the poor solubility of Slo-tail GST-fusion proteins.

Is the Ca^{2+} Bowl a Binding Site In Vivo?

The observation described above raises the issue of whether the Ca^{2+} bowl is a Ca^{2+}-binding site at all in the native channel. Or does it bind Ca^{2+} only after being subjected to SDS-PAGE and electroblotting? From our data we cannot answer this question definitively; however, we think that our observations that the same subregion of the Ca^{2+} bowl is important for both Ca^{2+} sensing and Ca^{2+} binding and that Ca^{2+} sensing depends on two negatively charged residues separated by one less critical residue—a common component of both EF-hand and C2 type Ca^{2+} binding sites (Falke et al., 1994; Nalefski and Falke, 1996)—tips the balance in favor of the hypothesis that this region forms a functionally relevant Ca^{2+}-binding site in vivo.

But if this is the case, how can we explain the results of Piskorowski and Aldrich (2002), who found that this part of the channel—and in fact the channel's entire intracellular domain—is not needed for Ca^{2+} sensing? The answer to this question is not apparent, although it could be that there are Ca^{2+}-binding sites in the channel's integral-membrane domain that are unrelated to the Ca^{2+} bowl and responsible for the Ca^{2+} sensitivity observed for the severely truncated channel (Pisko-

rowski and Aldrich, 2002). If this is the case, however, then such sites must be either uncovered upon truncation or disabled by mutations in the channel's intracellular domain, as mutations in this domain alone are sufficient to prevent Ca^{2+}-dependent activation (Fig. 1; Bao et al., 2002; Xia et al., 2002).

Bearing on this issue, Qian and Magleby (2003) have recently reported that when a channel carrying mutations in both its RCK domain and its Ca^{2+} bowl, and thus insensitive to micromolar Ca^{2+}, is expressed together with the BK_{Ca} β1 subunit, some Ca^{2+} sensitivity is restored to the channel. Since the β1 subunit does not appear to have Ca^{2+}-binding sites of its own (Qian and Magleby, 2003), this result argues either that the β1 subunit restores activity at the Ca^{2+}-binding sites disabled by the mutations, or that the β1 subunit uncovers dormant Ca^{2+}-binding sites. Perhaps, then, Ca^{2+} sensing in the BK_{Ca} channel can involve dormant sites that reside in the channel's integral membrane domain. To explain our results, however, no such a hypothesis is required.

Previous Biochemical Studies

Others have found before us that Ca^{2+} will bind to a fusion protein that contains amino acids that span the Ca^{2+} bowl. Braun and Sy (2001) observed, by gel-overlay assay, $^{45}Ca^{2+}$ binding to a recombinant mSlo peptide similar to the one we have used in our study, but they did not show that Ca^{2+}-bowl mutations could affect this binding. Bian et al. (2001), however, did make this connection. They found that Ca^{2+} would bind to a fusion protein that contained a 280–amino acid portion of *Drosophila* Slo (also by gel-overlay) and that this binding was inhibited by 56% when the Ca^{2+}-bowl residues 897–901 were mutated to asparagine. Thus, our results are consistent with these previous reports, although they may be distinguished in three respects. First, our most effective mutation in the binding assay D898A/D900A inhibited Ca^{2+} binding to a larger extent than did the 897–901N mutation of Bian et al. (2001) (80% compared with 56%). Second, Bian et al. (2001) examined only one mutation in their binding and electrophysiological assays, thus they were not likely to see the inconsistencies we have observed. And third, our mutations D898A and D900A much more effectively altered Ca^{2+} sensing than did theirs. In fact, in their study it was not apparent that their 897–901N mutation decreased the change in $V_{1/2}$ normally observed as $[Ca^{2+}]$ is increased. This latter difference, however, likely arises because their mutant still contained functioning high-affinity Ca^{2+}-binding sites of the second (RCK-associated) type (Bao et al., 2002; Xia et al., 2002), and because the Ca^{2+} concentrations they used were high enough to activate the channel's low-affinity Ca^{2+}-binding sites (Shi and Cui, 2001; Zhang et al., 2001; Bao et al., 2002; Shi et al., 2002). Thus, a direct comparison is perhaps not warranted. Nevertheless, Bian et al. (2001) interpreted their data to indicate a loss of function at a Ca^{2+}-bowl–related Ca^{2+}-binding site, an interpretation that we think is correct.

Previous Electrophysiological Studies

As mentioned above, because we have taken steps to minimize interference from the BK_{Ca} channel's RCK-associated high-affinity Ca^{2+}-binding sites and its low-affinity sites, it is often difficult to directly compare the electrophysiological data presented here to previous results; however, in the main, they appear consistent. Schreiber and Salkoff (1997), in the paper that defined the Ca^{2+} bowl, described five mutations (D898N, 897–899N, 897–901N, Δ897–898, Δ897–899) that altered channel gating in manner that they interpreted to indicate loss of function at the Ca^{2+} bowl. This interpretation has been further supported for the 897–901N mutant by three other studies (Bian et al., 2001; Niu and Magleby, 2002; Xia et al., 2002). All of these mutants contain mutations at 898 or at both 898 and 900, as is consistent with our data. We found in a previous study that the mutations Δ896–903, Δ898–903, and Δ899–903 could each eliminate Ca^{2+} bowl function (Bao et al., 2002), and again each contains a mutation at position 898 or 900 or both. And Braun and Sy (2001) found that a mutation at position 895 reduces the channel's response to Ca^{2+} but does not eliminate it, and we have observed a similar partial loss of Ca^{2+} sensitivity. No other Ca^{2+}-bowl mutations have been reported.

Conclusion

Here we have presented the first systematic analysis of the side chains of the Ca^{2+} bowl that are most important for Ca^{2+} sensing, We have narrowed the functionally relevant region of the Ca^{2+} bowl from 28 to ∼10 central residues, and we have shown that the many acidic residues in this central region are not functionally equivalent. Also, we have found that Ca^{2+} will bind to a peptide composed of GST and a 207–amino acid part of the mSlo tail that includes the Ca^{2+} bowl and that mutations that eliminate Ca^{2+} sensing via the Ca^{2+}-bowl–related site also greatly attenuate Ca^{2+} binding. Inconsistencies between our binding and electrophysiological data, however, have caused us to question whether the Ca^{2+} bowl is in a native conformation in our gel-overlay assay, and thus they suggest caution in using this assay to study Ca^{2+} binding at the Ca^{2+} bowl.

We gratefully acknowledge Dr. Andrew Braun for the generous gift of his GST-mSlo fusion-protein construct as well as a great deal of technical advice, Dr. Jim Baleja for his structural modeling of the Ca^{2+} bowl (Fig. 10), Dr. Christopher Schmid for statistical advice, Dr. Christopher Miller for helpful discussions, and Dr. Kathleen Dunlap, Dr. Robert Blaustein, and Anne Rapin for helpful comments on the manuscript.

This work was supported by grant R01HL64831 from the National Institutes of Health and by a grant from The Jessie B. Cox Charitable Trust and The Medical Foundation.

Olaf S. Andersen served as editor.

Submitted: 3 March 2004
Accepted: 6 April 2004

REFERENCES

Adelman, J.P., K.Z. Shen, M.P. Kavanaugh, R.A. Warren, Y.N. Wu, A. Lagrutta, C.T. Bond, and R.A. North. 1992. Calcium-activated potassium channels expressed from cloned complementary DNAs. *Neuron.* 9:209–216.

Atkinson, N.S., G.A. Robertson, and B. Ganetzky. 1991. A component of calcium-activated potassium channels encoded by the *Drosophila slo* locus. *Science.* 253:551–555.

Babu, A., H. Su, and J. Gulati. 1993. The mechanism of Ca^{2+}-coordination in the EF-hand of TnC, by cassette mutagenesis. *Adv. Exp. Med. Biol.* 332:125–131.

Babu, A., H. Su, Y. Ryu, and J. Gulati. 1992. Determination of residue specificity in the EF-hand of troponin C for Ca^{2+} coordination, by genetic engineering. *J. Biol. Chem.* 267:15469–15474.

Bandyopadhyay, J., J. Lee, J.I. Lee, J.R. Yu, C. Jee, J.H. Cho, S. Jung, M.H. Lee, S. Zannoni, A. Singson, et al. 2002. Calcineurin, a calcium/calmodulin-dependent protein phosphatase, is involved in movement, fertility, egg laying, and growth in *Caenorhabditis elegans. Mol. Biol. Cell.* 13:3281–3293.

Bao, L., A.M. Rapin, E.C. Holmstrand, and D.H. Cox. 2002. Elimination of the BK(Ca) channel's high-affinity Ca^{2+} sensitivity. *J. Gen. Physiol.* 120:173–189.

Barrett, J.N., K.L. Magleby, and B.S. Pallotta. 1982. Properties of single calcium-activated potassium channels in cultured rat muscle. *J. Physiol.* 331:211–230.

Bers, D., C. Patton, and R. Nuccitelli. 1994. A practical guide to the preparation of Ca buffers. *Methods Cell Biol.* 40:3–29.

Bian, S., I. Favre, and E. Moczydlowski. 2001. Ca^{2+}-binding activity of a COOH-terminal fragment of the *Drosophila* BK channel involved in Ca^{2+}-dependent activation. *Proc. Natl. Acad. Sci. USA.* 98:4776–4781.

Braun, A.F., and L. Sy. 2001. Contribution of potential EF hand motifs to the calcium-dependent gating of a mouse brain large conductance, calcium-sensitive K^+ channel. *J. Physiol.* 533:681–695.

Butler, A., S. Tsunoda, D.P. McCobb, A. Wei, and L. Salkoff. 1993. mSlo, a complex mouse gene encoding "maxi" calcium-activated potassium channels. *Science.* 261:221–224.

Cox, D.H., and R.W. Aldrich. 2000. Role of the beta1 subunit in large-conductance Ca^{2+}-activated K^+ channel gating energetics. Mechanisms of enhanced Ca^{2+} sensitivity. *J. Gen. Physiol.* 116: 411–432.

Cox, D.H., J. Cui, and R.W. Aldrich. 1997. Allosteric gating of a large conductance Ca-activated K^+ channel. *J. Gen. Physiol.* 110: 257–281.

Cui, J., and R.W. Aldrich. 2000. Allosteric linkage between voltage and Ca^{2+}-dependent activation of BK-type mslo1 K^+ channels. *Biochemistry.* 39:15612–15619.

Diaz, F., M. Wallner, E. Stefani, L. Toro, and R. Latorre. 1996. Interaction of internal Ba^{2+} with a cloned Ca^{2+}-dependent K^+ (hslo) channel from smooth muscle. *J. Gen. Physiol.* 107:399–407.

Dietrich, B. 1985. Coordination chemistry of alkali and alkali-earth cations with macrocyclic ligands. *J. Chem. Ed.* 62:954–964.

Falke, J.J., S.K. Drake, A.L. Hazard, and O.B. Peersen. 1994. Molecular tuning of ion binding to calcium signaling proteins. *Q. Rev. Biophys.* 27:219–290.

Hamill, O.P., A. Marty, E. Neher, B. Sakmann, and F.J. Sigworth. 1981. Improved patch-clamp techniques for high-resolution current recording from cells and cell-free membrane patches. *Pflugers Arch.* 391:85–100.

Hammarberg, T., P. Provost, B. Persson, and O. Radmark. 2000. The N-terminal domain of 5-lipoxygenase binds calcium and mediates calcium stimulation of enzyme activity. *J. Biol. Chem.* 275: 38787–38793.

Horrigan, F.T., and R.W. Aldrich. 1999. Allosteric voltage gating of potassium channels II. Mslo channel gating charge movement in the absence of Ca^{2+}. *J. Gen. Physiol.* 114:305–336.

Horrigan, F.T., and R.W. Aldrich. 2002. Coupling between voltage sensor activation, Ca^{2+} binding and channel opening in large conductance (BK) potassium channels. *J. Gen. Physiol.* 120:267–305.

Horrigan, F.T., J. Cui, and R.W. Aldrich. 1999. Allosteric voltage gating of potassium channels I. Mslo ionic currents in the absence of Ca^{2+}. *J. Gen. Physiol.* 114:277–304.

Jegerschold, C., A.W. Rutherford, T.A. Mattioli, M. Crimi, and R. Bassi. 2000. Calcium binding to the photosystem II subunit CP29. *J. Biol. Chem.* 275:12781–12788.

Jiang, Y., A. Lee, J. Chen, M. Cadene, B.T. Chait, and R. MacKinnon. 2002. Crystal structure and mechanism of a calcium-gated potassium channel. *Nature.* 417:515–522.

Jiang, Y., A. Lee, J. Chen, V. Ruta, M. Cadene, B.T. Chait, and R. MacKinnon. 2003. X-ray structure of a voltage-dependent K^+ channel. *Nature.* 423:33–41.

Jiang, Y., A. Pico, M. Cadene, B.T. Chait, and R. MacKinnon. 2001. Structure of the RCK domain from the E. coli K^+ channel and demonstration of its presence in the human BK channel. *Neuron.* 29:593–601.

Latorre, R., A. Oberhauser, P. Labarca, and O. Alvarez. 1989. Varieties of calcium-activated potassium channels. *Annu. Rev. Physiol.* 51:385–399.

Maruyama, K., T. Mikawa, and S. Ebashi. 1984. Detection of calcium binding proteins by ^{45}Ca autoradiography on nitrocellulose membrane after sodium dodecyl sulfate gel electrophoresis. *J. Biochem. (Tokyo).* 95:511–519.

Menguy, T., F. Corre, L. Bouneau, S. Deschamps, J.V. Moller, P. Champeil, M. le Maire, and P. Falson. 1998. The cytoplasmic loop located between transmembrane segments 6 and 7 controls activation by Ca^{2+} of sarcoplasmic reticulum Ca^{2+}-ATPase. *J. Biol. Chem.* 273:20134–20143.

Methfessel, C., and G. Boheim. 1982. The gating of single calcium-dependent potassium channels is described by an activation/blockade mechanism. *Biophys. Struct. Mech.* 9:35–60.

Morohashi, Y., N. Hatano, S. Ohya, R. Takikawa, T. Watabiki, N. Takasugi, Y. Imaizumi, T. Tomita, and T. Iwatsubo. 2002. Molecular cloning and characterization of CALP/KChIP4, a novel EF-hand protein interacting with presenilin 2 and voltage-gated potassium channel subunit Kv4. *J. Biol. Chem.* 277:14965–14975.

Nalefski, E.A., and J.J. Falke. 1996. The C2 domain calcium-binding motif: structural and functional diversity. *Protein Sci.* 5:2375–2390.

Ngai, P.K., G.C. Scott-Woo, M.S. Lim, C. Sutherland, and M.P. Walsh. 1987. Activation of smooth muscle myosin Mg^{2+}-ATPase by native thin filaments and actin/tropomyosin. *J. Biol. Chem.* 262:5352–5359.

Niu, X., and K.L. Magleby. 2002. Stepwise contribution of each subunit to the cooperative activation of BK channels by Ca^{2+}. *Proc. Natl. Acad. Sci. USA.* 99:11441–11446.

Pallanck, L., and B. Ganetzky. 1994. Cloning and characterization of human and mouse homologs of the *Drosophila* calcium-activated potassium channel gene, slowpoke. *Hum. Mol. Genet.* 3:1239–1243.

Perisic, O., S. Fong, D.E. Lynch, M. Bycroft, and R.L. Williams. 1998. Crystal structure of a calcium-phospholipid binding do-

main from cytosolic phospholipase A2. *J. Biol. Chem.* 273:1596–1604.

Piskorowski, R., and R.W. Aldrich. 2002. Calcium activation of BK_{Ca} potassium channels lacking the calcium bowl and RCK domains. *Nature.* 420:499–502.

Qian, X., and K.L. Magleby. 2003. Beta1 subunits facilitate gating of BK channels by acting through the Ca^{2+}, but not the Mg^{2+}, activating mechanisms. *Proc. Natl. Acad. Sci. USA.* 100:10061–10066.

Rajini, B., P. Shridas, C.S. Sundari, D. Muralidhar, S. Chandani, F. Thomas, and Y. Sharma. 2001. Calcium binding properties of gamma-crystallin: calcium ion binds at the Greek key βγ-crystallin fold. *J. Biol. Chem.* 276:38464–38471.

Rothberg, B.S., and K.L. Magleby. 2000. Voltage and Ca^{2+} activation of single large-conductance Ca^{2+}-activated K+ channels described by a two-tiered allosteric gating mechanism. *J. Gen. Physiol.* 116:75–99.

Schreiber, M., and L. Salkoff. 1997. A novel calcium-sensing domain in the BK channel. *Biophys. J.* 73:1355–1363.

Schreiber, M., A. Yuan, and L. Salkoff. 1999. Transplantable sites confer calcium sensitivity to BK channels. *Nat. Neurosci.* 2:416–421.

Shen, K.Z., A. Lagrutta, N.W. Davies, N.B. Standen, J.P. Adelman, and R.A. North. 1994. Tetraethylammonium block of Slowpoke calcium-activated potassium channels expressed in Xenopus oocytes: evidence for tetrameric channel formation. *Pflugers Arch.* 426:440–445.

Shi, J., and J. Cui. 2001. Intracellular Mg^{2+} enhances the function of BK-type Ca^{2+}-activated K^+ channels. *J. Gen. Physiol.* 118:589–606.

Shi, J., G. Krishnamoorthy, Y. Yang, L. Hu, N. Chaturvedi, D. Harilal, J. Qin, and J. Cui. 2002. Mechanism of magnesium activation of calcium-activated potassium channels. *Nature.* 418:876–880.

Sienaert, I., L. Missiaen, H. De Smedt, J.B. Parys, H. Sipma, and R. Casteels. 1997. Molecular and functional evidence for multiple Ca^{2+}-binding domains in the type 1 inositol 1,4,5-trisphosphate receptor. *J. Biol. Chem.* 272:25899–25906.

Tompa, P., Y. Emori, H. Sorimachi, K. Suzuki, and P. Friedrich. 2001. Domain III of calpain is a Ca^{2+}-regulated phospholipid-binding domain. *Biochem. Biophys. Res. Commun.* 280:1333–1339.

Wei, A., C. Solaro, C. Lingle, and L. Salkoff. 1994. Calcium sensitivity of BK-type K_{Ca} channels determined by a separable domain. *Neuron.* 13:671–681.

Xia, X.M., X. Zeng, and C.J. Lingle. 2002. Multiple regulatory sites in large-conductance calcium-activated potassium channels. *Nature.* 418:880–884.

Zhang, X., C.R. Solaro, and C.J. Lingle. 2001. Allosteric regulation of BK channel gating by Ca^{2+} and Mg^{2+} through a nonselective, low affinity divalent cation site. *J. Gen. Physiol.* 118:607–636.